




Cite this: *RSC Adv.*, 2022, 12, 23411

# Functionalization of a stable AIE-based hydrogen-bonded organic framework for white light-emitting diodes†

Yu-Xin Lin, Jia-Xin Wang,  Cong-Cong Liang,  \* Chenghao Jiang, Bin Li  and Guodong Qian 

Hydrogen-bonded organic frameworks (HOFs) have received tremendous attention in recent years due to the good designability. However, the pure organic nature of HOFs sometimes limits the application development and performance improvement. Functionalizing is an effective strategy to control and modulate material properties, which can achieve properties that cannot be achieved by a pristine material. Herein, a series of HOF-76 $\supset$ DSMI were synthesized through functionalizing the stable AIE-based HOF-76 by incorporating a red dye which complements the deficiency of the red component of HOF-76. Then, a single matrix white light-emitting diode (WLED) was fabricated by coating the HOF-76 $\supset$ DSMI material on a 460 nm blue LED with CIE chromaticity coordinates of (0.333, 0.329), a correlated colour temperature (CCT) of 5490 K and a colour rendering index (CRI) of 80.

Received 14th July 2022  
Accepted 10th August 2022

DOI: 10.1039/d2ra04342d

rsc.li/rsc-advances

## Introduction

Hydrogen-bonded organic frameworks (HOFs), an emerging type of porous crystalline material, are assembled of organic linkers through hydrogen bonding and have attracted continuous attention.<sup>1–4</sup> The variability of the hydrogen bond distance and angle give HOFs unique features compared with other porous crystalline materials, including but not limited to mild synthesis conditions, easy regeneration and high thermal stability.<sup>5–9</sup> Until now, the structural design of HOFs has matured to a point in which the composition, structure, and porosity can be precisely designed<sup>10–12</sup> and they show outstanding properties in many fields such as gas separation,<sup>13–16</sup> sensors,<sup>17–19</sup> catalysis,<sup>20–22</sup> proton conduction,<sup>23,24</sup> luminescent materials,<sup>25–28</sup> *etc.* However, the lack of functional sites limits functional development and performance breakthroughs of HOFs to some extent.

Functionalizing materials is an important material design strategy for specific applications.<sup>29–32</sup> Strong Lewis base/acid sites or other functional groups can be incorporated into HOF precursors for compatibility with special applications. For example, pyridyl, hydroxyl and F atoms are considered functional groups that can recognize small molecules specifically.<sup>33,34</sup> Jiang and Chen *et al.* constructed a post-synthetic

metallized HOF-19 with palladium acetate exhibiting high isolation yields and good selectivity for the Suzuki–Miyaura coupling reaction.<sup>20</sup> Farha and co-workers reported post-synthetic incorporation of iodine within conductive HOF-110 affording a 30-fold improvement in electrical conductivity.<sup>35</sup> Sun and Luo *et al.* proposed to load the doxorubicin onto the surface of a porphyrin-based HOF, which provided synergistic chemotherapy–photodynamic therapy–photothermal therapy effects.<sup>36</sup> These works inspire us to construct functionalized HOFs for the application of white light-emitting diodes (WLEDs) which is difficult to be achieved by a HOF material itself.<sup>37,38</sup>

Herein, we report a series of functionalized aggregation-induced emission-based (AIE-based) HOFs (HOF-76 $\supset$ DSMI) by introducing a dye molecule into the HOF-76 host which is constructed from an AIE linker hexakis(4-carboxyphenylethynyl)-benzene (HCEB). The emission of HOF-76 $\supset$ DSMI materials undergoes a change from single green emission to red emission with the variation of dye molecule loading amount. Among them, HOF-76 $\supset$ DSMI@0.22 wt% shows a high-quality pure white light excited by a 460 nm blue LED chip and a single matrix WLED was fabricated.

## Results and discussion

### AIE character of HCEB

We first demonstrated the AIE character of the HCEB and investigated the effect of the HOF framework structure on the photoluminescent (PL) properties. The compound HCEB was successfully synthesized according to the published procedure.<sup>39</sup> As shown in Fig. 1a, the solid ligand HCEB exhibits

State Key Laboratory of Silicon Materials, School of Materials Science & Engineering, Zhejiang University, Hangzhou, 310027, China. E-mail: liangcc1@zju.edu.cn; bin.li@zju.edu.cn

† Electronic supplementary information (ESI) available: Experimental section (measurements, synthesis and calculation); additional graphics (Fig. S1–S11) and table (Table S1). See <https://doi.org/10.1039/d2ra04342d>



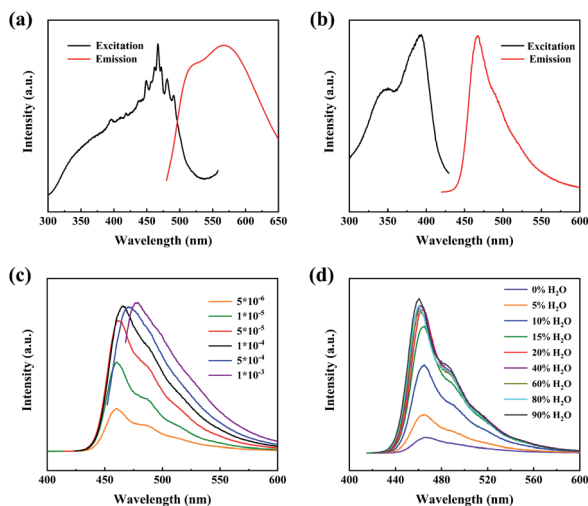


Fig. 1 PL spectra of (a) HCEB powder and (b) HCEB solution in DMSO (10  $\mu$ M). (c) The emission spectra of HCEB in DMSO with different concentrations. (d) The emission spectra of HCEB solution (10  $\mu$ M) in a mixture of DMSO/water with different water fractions.

a broad yellow emission of 500–650 nm under a wide excitation range of 400–500 nm. The dilute solution of HCEB in DMSO can be excited by UV light and the maximum emission peak is 466 nm (Fig. 1b) but the intensity is very weak. When the concentration of HCEB ligand increases, the emission intensity gradually enhances and the emission peak redshift (Fig. 1c), which is attributed to the formation of excimers.<sup>40–43</sup> On the other hand, we added poor solvent H<sub>2</sub>O into the dilute solution and observed the emission intensity also increases sharply (Fig. 1d and S1a, ESI<sup>†</sup>). When mixing a 90% volume fraction of water in DMSO, the absorption peak of HCEB suspension in the DMSO/H<sub>2</sub>O mixture remains unchanged (Fig. S1b, ESI<sup>†</sup>), while the emission peak is significantly blue-shifted ( $\lambda_{\text{max}} = 466$  nm in DMSO;  $\lambda_{\text{max}} = 459$  nm in DMSO/H<sub>2</sub>O; see Fig. 1d). This intriguing aggregation-induced blue-shifted emission can ascribe to the presence of water molecules weakly blocking the intramolecular/intermolecular excited aromatic interactions in the aggregated state.<sup>44,45</sup> The AIE character of HCEB molecular indicates the feasibility of constructing high quantum efficiency luminescent HOFs.

### Rigidifying the linkers by HOF formation

HOF-76 crystal was successfully synthesized with an HCEB ligand.<sup>39</sup> The powder X-ray diffraction patterns show the pure phase and good crystallinity of HOF-76 (Fig. 2a). The quantum efficiency of HOF-76 is 9.76% that is higher than that of the HCEB ligand (2.59%), which proved the successful restriction of AIE HCEB ligand by hydrogen bond and  $\pi$ - $\pi$  interaction in HOF-76. The restriction inhibits the motion of the benzene ring and the internal torsion of the alkyne group thus blocks the non-radiation transition and reverses the path of radiation transition which leads to a luminescence intensity increase of molecule.<sup>46</sup> HOF-76 exhibits a green emission at  $\lambda_{\text{max}} = 508$  nm and two distinct reddish emission peaks around 550–600 nm

(Fig. 2b). To further explore the role of crystal structure in the photoluminescence of HOF-76, we investigated the UV-vis absorption spectra and emission spectra of HOF-76 and the single-molecular state ligand (Fig. S2, ESI<sup>†</sup>) respectively. The absorption spectra show the strongest absorption peak located at 326 nm and 362 nm for HOF-76 and single-molecular state ligand (Fig. S2a, ESI<sup>†</sup>), respectively, which can be regarded as S0  $\rightarrow$  S2 transition. However, a broad absorption peak around 400–500 nm was observed for HOF-76 but non for the single-molecular state, which is corresponding to the 0–0 transition for S0  $\rightarrow$  S1.<sup>47–49</sup> The restriction of H-bonds in HOF-76 breaks the original  $D_{6h}$  symmetry of ligand, therefore, allowing the 0–0 transition.<sup>48</sup> Furthermore, the emission spectrum of HOF-76 exhibits a bathochromic shift of 31 nm compared with the single-molecular state of HCEB in 80 K (Fig. S2b, ESI<sup>†</sup>), which is caused by  $\pi$ - $\pi$  stacking and the photoinduced proton transfer among the H-bonds between carboxyl groups.<sup>49</sup> Therefore, crystal engineering is an efficient strategy to modulate the luminescence properties of molecules.

### Synthesis and photophysical properties of HOF-76 $\supset$ DSMI

For the pore structure and luminescence properties of HOF-76, we choose the DSMI dye molecule as the functional guest molecule for several reasons (Scheme 1): (1) HOF-76 and DSMI show the same optical excitation wavelength and can be excited by 460 nm simultaneously. DSMI emits red light at  $\lambda_{\text{max}} = 625$  nm which complements the deficiency of the red component of HOF-76 (Fig. 2c). (2) The molecular dimension of DSMI is  $\sim 4.3 \times 15.9$  Å<sup>2</sup> and smaller than the aperture of the 1D channel of the HOF-76 (7 Å). Thus, the dye molecules could easily enter the pore of HOF-76. (3) The interaction between cationic DSMI and benzene ring electron clouds can make the guest molecule encapsulated within the HOF-76 pores.

Activated HOF-76 crystals (Fig. S3, ESI<sup>†</sup>) were immersed in aqueous DSMI solution and kept for three days at room temperature to ensure the system was fully balanced. A series of functionalized HOF-76 (HOF-76  $\supset$  DSMI) were obtained without structural collapsing (Fig. 2a and S3, S4, ESI<sup>†</sup>). The fluorescence microscope photos further proved the uniformly loading of DSMI in HOF-76 crystals (Fig. 2e and f) and the variation of luminous colour suggested the emission colour be tuned by controlling the loading amount of DSMI. The loading amount of DSMI was calculated by the intensity-concentration relationship of the UV-vis absorption spectra (Fig. S5 and S6, ESI<sup>†</sup>) and its maximum value is 1.42 wt%. Next, we measured the emission spectra of this series of HOF-76  $\supset$  DSMI. The materials display continuous broadband emission and a new emission band appears at around 600 nm compared with HOF-76 (Fig. 2d), which revealed the modulation of fluorescence property is successfully achieved by functionalizing HOF-76. As expected, the emission intensity of the green component of the emission spectra decreases with the increase in loading amount. This is attributed to the efficient energy/charge transfer between the host HOF-76 framework and guest DSMI molecule, which is proved by the overlapping of the emission spectrum for HOF-76 and absorption spectrum for DSMI



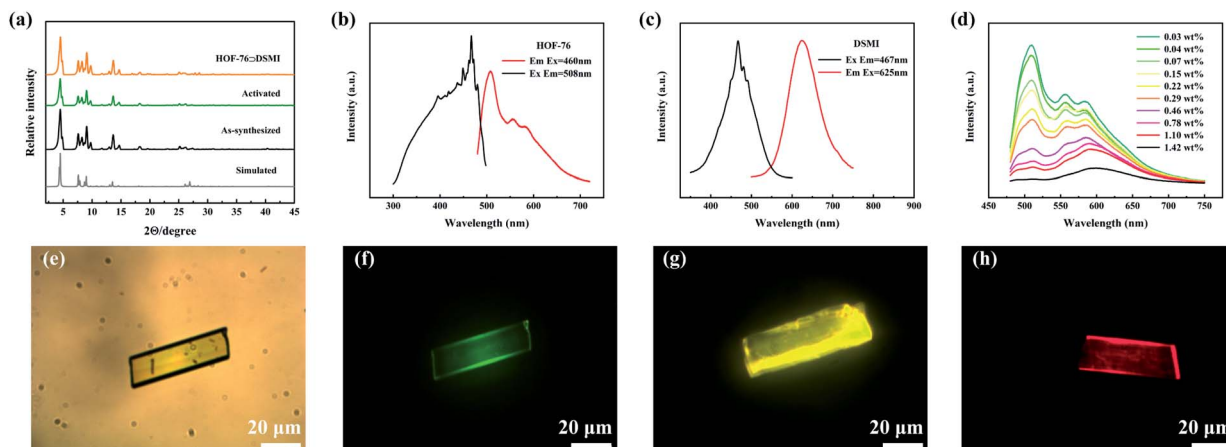
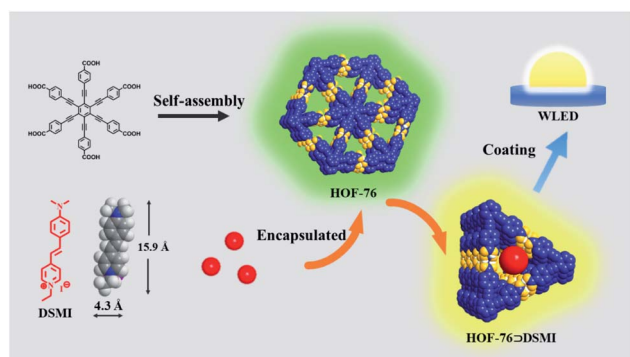


Fig. 2 (a) Powder X-ray diffraction patterns of as-synthesized and activated HOF-76 and HOF-76@DSMI compared with simulated diffraction pattern of single-crystal HOF-76. PL spectra of (b) HOF-76 and (c)  $1 \times 10^{-5}$  M DSMI in DMF solution. (d) The emission spectra of HOF-76@DSMI with different loading amounts of DSMI. All samples were excited at the wavelength of 460 nm. (e) The microscope of HOF-76. The fluorescence microscopic image under the excitation of 480 nm of (f) HOF-76 (g) HOF-76@DSMI@0.22 wt% (h) HOF-76@DSMI@1.42 wt%.



Scheme 1 Schematic illustration of the design and synthesis of HOF-76@DSMI and the packaging of a WLED.

(Fig. 2b and S6a, ESI<sup>†</sup>). Thus, we further measured the quantum yield of these series of functionalized HOF-76 materials. Indeed, it is consistent that the existence of DSMI leads to the reduction of quantum efficiency (Table S1 and Fig. S7, ESI<sup>†</sup>). Such a HOF-to-dye energy transfer behaviour was further evidenced by emission spectrum and the lifetime measurement by time-resolved PL decay experiments (Fig. S8 and S9, ESI<sup>†</sup>).

We collected the decay curves at 510 nm excited under a continuous laser at 470 nm. The lifetime of each sample is summarized in Table S1 (ESI<sup>†</sup>). HOF-76 exhibits substantial bi-exponential decay photo-behaviour with a shorter lifetime  $\tau_1$  of 5.63 ns and a longer lifetime  $\tau_2$  of 14.94 ns. The longer lifetime is attributed to the lifetime of the luminescent nucleus, substituents and their interactions have little effect. The shorter lifetime is attributed to charge transfer between carboxylic groups.<sup>47</sup> With the increase in the loading amount of DSMI, the luminescence and lifetime of the material decrease. Thus, it can be assigned to the energy transfer occurred in the host-guest system, which gives rise to increase non-radiative decay. The calculated energy transfer efficiency  $\eta$  is approximately 31.1% with 0.22 wt% DSMI loading amount.<sup>50,51</sup> The great energy level

match between the S1 level of the HOF-76 and DSMI is further confirmed by steady-state spectra (Fig. S10, ESI<sup>†</sup>). Therefore, it is answerable to the gradually quenched green light of HOF-76@DSMI near 508 nm. The luminescence spectrum of HOF-76@DSMI@1.42 wt% is consistent with the emission of DSMI (Fig. 2d). However, the quantum yield of HOF-76@DSMI@1.42 wt% (2.63%) is much higher than that of DSMI powder (<1%), which indicates that the confinement effect of the HOF-76 on the DSMI molecules inhibits the aggregation of the DSMI and therefore enhances the quantum yield.

### Fabrication of the WLED

The emission of HOF-76@DSMI materials shift from green light toward red light as the loading amount increased, which is illustrated by the chromatic coordinate diagram (Fig. S11, ESI<sup>†</sup>). Surprisingly, the CIE coordination of HOF-76@DSMI@0.22 wt% (0.41, 0.52) is comparatively close to commercial yellow phosphor YAG : Ce<sup>3+</sup> (0.41, 0.56). Encouraged by this result, to further demonstrate the capacity of the functionalizing HOFs for practical white-light emitting applications, we produced a white emitting device by implementing HOF-76@DSMI@0.22 wt% as yellow phosphor onto the 460 nm blue LED with hemispherical morphology. The emission spectrum of device was recorded by fibre optical spectrometer. As shown in Fig. 3a, a broadband emission covering the whole visible spectral region was achieved and the result remote-type LED device emits a bright white light when is connected to the electrical power of 3 V. The white light was obtained with CIE coordinates of (0.333, 0.329), as depicted in the CIE 1931 chromaticity diagram (Fig. 3b), which is closed to standard commercial white light (CIE coordinates = 0.33, 0.33). The calculated CCT value of 5490 K is much lower than commercial blue-LED chip excited YAG : Ce<sup>3+</sup> phosphor (CCT = 6015 K). It is obvious that compensating for the deficiency of the red component is manifested in HOF-76@DSMI, which is more comfortable for people in daily life.<sup>52</sup> The measured



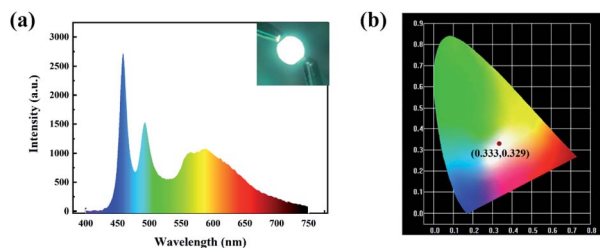


Fig. 3 (a) The emission spectrum of WLED after loading the HOF-76⊃DSMI onto 460 nm blue chip; inset: the photo of the obtained WLED when applying the current. (b) CIE chromaticity coordinates of as-fabricated WLED.

corresponding colour rendering index (CRI) value is 80, completely meeting the requirements of white light performance.

## Conclusions

In summary, we functionalized the stable AIE-based HOF-76 by loading DSMI red dye, making it an efficient yellow phosphor that cannot be achieved by pure HOF-76 itself. A WLED with CIE coordinates of (0.333, 0.329), CCT of 5490 K and CRI of 80 was constructed by combining the phosphor with accessible commercial blue LED chip. All indicators show the colour rendering ability of the phosphors satisfying people's demands and display a potential application in warm-white light LEDs. What's more, to the best of our knowledge, this is the first reported WLED that the phosphor is constructed by a functionalized AIE-based HOF, which expands the application of HOF materials in the optical field.

## Conflicts of interest

There are no conflicts to declare.

## Acknowledgements

This work was supported by the National Science Foundation of China (52073251), and the Zhejiang Provincial Natural Science Foundation of China (No. LR22E030003).

## Notes and references

- B. Wang, R. Lin, Z. Zhang, S. Xiang and B. Chen, *J. Am. Chem. Soc.*, 2020, **142**, 14399.
- X. Song, Y. Wang, C. Wang, D. Wang, G. Zhuang, K. O. Kirlikovali, P. Li and O. K. Farha, *J. Am. Chem. Soc.*, 2022, **144**, 10663–10687.
- L. Chen, B. Zhang, L. Chen, H. Liu, Y. Hu and S. Qiao, *Materials Advances*, 2022, **3**, 3680.
- Y. He, S. Xiang and B. Chen, *J. Am. Chem. Soc.*, 2011, **133**, 14570.
- R. Lin, Y. He, P. Li, H. Wang, W. Zhou and B. Chen, *Chem. Soc. Rev.*, 2019, **48**, 1362.
- I. Hisaki, C. Xin, K. Takahashi and T. Nakamura, *Angew. Chem., Int. Ed.*, 2019, **58**, 11160.
- Q. Huang, W. Li, Z. Mao, L. Qu, Y. Li, H. Zhang, T. Yu, Z. Yang, J. Zhao, Y. Zhang, M. P. Aldred and Z. Chi, *Nat. Commun.*, 2019, **10**, 3074.
- X. Luo, X. Jia, J. Deng, J. Zhong, H. Liu, K. Wang and D. Zhong, *J. Am. Chem. Soc.*, 2013, **135**, 11684.
- F. Hu, C. Liu, M. Wu, J. Pang, F. Jiang, D. Yuan and M. Hong, *Angew. Chem., Int. Ed.*, 2017, **56**, 2101.
- A. Pulido, L. Chen, T. Kaczorowski, D. Holden, M. A. Little, S. Y. Chong, B. J. Slater, D. P. McMahon, B. Bonillo, C. J. Stackhouse, A. Stephenson, C. M. Kane, R. Clowes, T. Hasell, A. I. Cooper and G. M. Day, *Nature*, 2017, **543**, 657.
- P. Li, P. Li, M. R. Ryder, Z. Liu, C. L. Stern, O. K. Farha and J. F. Stoddart, *Angew. Chem., Int. Ed.*, 2019, **58**, 1664.
- M. Mastalerz and I. M. Oppel, *Angew. Chem., Int. Ed.*, 2012, **51**, 5252.
- X. Zhang, J. Wang, L. Li, J. Pei, R. Krishna, H. Wu, W. Zhou, G. Qian, B. Chen and B. Li, *Angew. Chem., Int. Ed.*, 2021, **60**, 10304.
- Y. Yang, L. Li, R. Lin, Y. Ye, Z. Yao, L. Yang, F. Xiang, S. Chen, Z. Zhang, S. Xiang and B. Chen, *Nat. Chem.*, 2021, **13**, 933.
- Y. Li, E. V. Alexandrov, Q. Yin, L. Li, Z. Fang, W. Yuan, D. M. Proserpio and T. Liu, *J. Am. Chem. Soc.*, 2020, **142**, 7218.
- T. Chen, I. Popov, W. Kaveevivitchai, Y. Chuang, Y. Chen, O. Daugulis, A. J. Jacobson and O. Š. Miljanić, *Nat. Commun.*, 2014, **5**, 5131.
- B. Wang, R. He, L. Xie, Z. Lin, X. Zhang, J. Wang, H. Huang, Z. Zhang, K. S. Schanze, J. Zhang, S. Xiang and B. Chen, *J. Am. Chem. Soc.*, 2020, **142**, 12478.
- I. Hisaki, Y. Suzuki, E. Gomez, Q. Ji, N. Tohnai, T. Nakamura and A. Douhal, *J. Am. Chem. Soc.*, 2019, **141**, 2111.
- Y. Wang, D. Liu, J. Yin, Y. Shang, J. Du, Z. Kang, R. Wang, Y. Chen, D. Sun and J. Jiang, *Chem. Commun.*, 2020, **56**, 703.
- B. Han, H. Wang, C. Wang, H. Wu, W. Zhou, B. Chen and J. Jiang, *J. Am. Chem. Soc.*, 2019, **141**, 8737.
- J. Tang, J. Liu, Q. Zheng, W. Li, J. Sheng, L. Mao and M. Wang, *Angew. Chem., Int. Ed.*, 2021, **60**, 22315.
- W. Gong, D. Chu, H. Jiang, X. Chen, Y. Cui and Y. Liu, *Nat. Commun.*, 2019, **10**, 600.
- A. Karmakar, R. Illathvalappil, B. Anothumakkool, A. Sen, P. Samanta, A. V. Desai, S. Kurungot and S. K. Ghosh, *Angew. Chem.*, 2016, **128**, 10825.
- M. Wei, Y. Gao, K. Li, B. Li, J. Fu, H. Zang, K. Shao and Z. Su, *CrystEngComm*, 2019, **21**, 4996.
- L. Bian, H. Shi, X. Wang, K. Ling, H. Ma, M. Li, Z. Cheng, C. Ma, S. Cai, Q. Wu, N. Gan, X. Xu, Z. An and W. Huang, *J. Am. Chem. Soc.*, 2018, **140**, 10734.
- Q. Yin, P. Zhao, R. Sa, G. Chen, J. Lü, T. Liu and R. Cao, *Angew. Chem., Int. Ed.*, 2018, **57**, 7691.
- H. Zhang, D. Yu, S. Liu, C. Liu, Z. Liu, J. Ren and X. Qu, *Angew. Chem., Int. Ed.*, 2022, **61**, e202109068.
- Y. Lv, D. Li, A. Ren, Z. Xiong, Y. Yao, K. Cai, S. Xiang, Z. Zhang and Y. S. Zhao, *ACS Appl. Mater. Interfaces*, 2021, **13**, 28662.





- 29 L. Jiao, J. Y. R. Seow, W. S. Skinner, Z. U. Wang and H. Jiang, *Mater. Today*, 2019, **27**, 43.
- 30 M. D. Allendorf, M. E. Foster, F. Léonard, V. Stavila, P. L. Feng, F. P. Doty, K. Leong, E. Y. Ma, S. R. Johnston and A. A. Talin, *J. Phys. Chem. Lett.*, 2015, **6**, 1182.
- 31 G. Mínguez Espallargas and E. Coronado, *Chem. Soc. Rev.*, 2018, **47**, 533.
- 32 J. Pei, H. Wen, X. Gu, Q. Qian, Y. Yang, Y. Cui, B. Li, B. Chen and G. Qian, *Angew. Chem., Int. Ed.*, 2021, **60**, 25068.
- 33 H. Deng, C. J. Doonan, H. Furukawa, R. B. Ferreira, J. Towne, C. B. Knobler, B. Wang and O. M. Yaghi, *Science*, 2010, **327**, 846.
- 34 B. Wang, R. He, L. Xie, Z. Lin, X. Zhang, J. Wang, H. Hong, Z. Zhang, K. S. Schanze, J. Zhang, S. Xiang and B. Chen, *J. Am. Chem. Soc.*, 2020, **28**, 12478.
- 35 K. O. Kirlikovali, S. Goswami, M. R. Mian, M. D. Krzyaniak, M. R. Wasielewski, J. T. Hupp, P. Li and O. K. Farha, *ACS Mater. Lett.*, 2022, **4**, 128.
- 36 X. He, Y. Luo, D. Hong, F. Chen, Z. Zheng, C. Wang, J. Wang, C. Chen and B. Sun, *ACS Appl. Nano Mater.*, 2019, **2**, 2437.
- 37 X. Liu, K. Xing, Y. Li, C. Tsung and J. Li, *J. Am. Chem. Soc.*, 2019, **141**, 14807.
- 38 X. Liu, Y. Li, C. Tsung and J. Li, *Chem. Commun.*, 2019, **55**, 10669.
- 39 X. Zhang, L. Li, J. Wang, H. Wen, R. Krishna, H. Wu, W. Zhou, Z. Chen, B. Li, G. Qian and B. Chen, *J. Am. Chem. Soc.*, 2020, **142**, 633.
- 40 Y. Hong, J. W. Y. Lam and B. Z. Tang, *Chem. Soc. Rev.*, 2011, **40**, 5361.
- 41 J. Mei, N. L. C. Leung, R. T. K. Kwok, J. W. Y. Lam and B. Z. Tang, *Chem. Rev.*, 2015, **115**, 11718.
- 42 Z. Wei, Z. Gu, R. K. Arvapally, Y. Chen, R. N. McDougald, J. F. Ivy, A. A. Yakovenko, D. Feng, M. A. Omary and H. Zhou, *J. Am. Chem. Soc.*, 2014, **136**, 8269.
- 43 N. B. Shustova, B. D. McCarthy and M. Dincă, *J. Am. Chem. Soc.*, 2011, **133**, 20126.
- 44 J. Xiong, K. Wang, Z. Yao, B. Zou, J. Xu and X. Bu, *ACS Appl. Mater. Interfaces*, 2018, **10**, 5819.
- 45 Q. Wu, T. Zhang, Q. Peng, D. Wang and Z. Shuai, *Phys. Chem. Chem. Phys.*, 2014, **16**, 5545.
- 46 N. B. Shustova, T. Ong, A. F. Cozzolino, V. K. Michaelis, R. G. Griffin and M. Dincă, *J. Am. Chem. Soc.*, 2012, **134**, 15061.
- 47 H. Imoto, S. Tanaka, T. Kato, S. Watase, K. Matsukawa, T. Yumura and K. Naka, *Organometallics*, 2016, **35**, 364.
- 48 L. Fiedor, A. Dudkowiak and M. Pilch, *J. R. Soc., Interface*, 2019, **16**, 20190191.
- 49 E. Gomez, M. Gutiérrez, B. Cohen, I. Hisaki and A. Douhal, *J. Mater. Chem. C*, 2018, **6**, 6929.
- 50 C. Zhang, Z. Yan, X. Dong, Z. Han, S. Li, T. Fu, Y. Zhu, Y. Zheng, Y. Niu and S. Zang, *Adv. Mater.*, 2020, **32**, 2002914.
- 51 R. Sun, P. Lu, D. Zhou, W. Xu, N. Ding, H. Shao, Y. Zhang, D. Li, N. Wang, X. Zhuang, B. Dong, X. Bai and H. Song, *ACS Energy Lett.*, 2020, **5**, 2131.
- 52 X. Ma, X. Xu, F. Duan, W. Huang, Q. Chen and D. Wu, *Adv. Opt. Mater.*, 2022, **10**, 2101461.

